UNIVERSITY OF BIRMINGHAM
University of Birmingham Research at Birmingham

Electrophoretic deposition of organic/inorganic composite coatings containing ZnO nanoparticles exhibiting antibacterial properties

Karbowniczek, Joanna; Cordero-arias, Luis; Virtanen, Sannakaisa; Misra, Superb K.; Valsami-jones, Eugenia; Tuchscherr, Lorena; Rutkowski, Bogdan; Górecki, Kamil; Bała, Piotr; Czyrska-filemonowicz, Aleksandra; Boccaccini, Aldo R.

DOI:
10.1016/j.msec.2017.03.180

License:
Creative Commons: Attribution-NonCommercial-NoDerivs (CC BY-NC-ND)

Document Version
Peer reviewed version

Citation for published version (Harvard):
Karbowniczek, J, Cordero-arias, L, Virtanen, S, Misra, SK, Valsami-jones, E, Tuchscherr, L, Rutkowski, B, Górecki, K, Bała, P, Czyrska-filemonowicz, A & Boccaccini, AR 2017, 'Electrophoretic deposition of organic/inorganic composite coatings containing ZnO nanoparticles exhibiting antibacterial properties', *Materials Science and Engineering C*, vol. 77, pp. 780-789. https://doi.org/10.1016/j.msec.2017.03.180

Link to publication on Research at Birmingham portal

General rights
Unless a licence is specified above, all rights (including copyright and moral rights) in this document are retained by the authors and/or the copyright holders. The express permission of the copyright holder must be obtained for any use of this material other than for purposes permitted by law.

•Users may freely distribute the URL that is used to identify this publication.
•Users may download and/or print one copy of the publication from the University of Birmingham research portal for the purpose of private study or non-commercial research.
•User may use extracts from the document in line with the concept of 'fair dealing' under the Copyright, Designs and Patents Act 1988 (?)
•Users may not further distribute the material nor use it for the purposes of commercial gain.

Where a licence is displayed above, please note the terms and conditions of the licence govern your use of this document.

When citing, please reference the published version.

Take down policy
While the University of Birmingham exercises care and attention in making items available there are rare occasions when an item has been uploaded in error or has been deemed to be commercially or otherwise sensitive.

If you believe that this is the case for this document, please contact UBIRA@lists.bham.ac.uk providing details and we will remove access to the work immediately and investigate.

Download date: 19. Apr. 2024

Accepted Manuscript

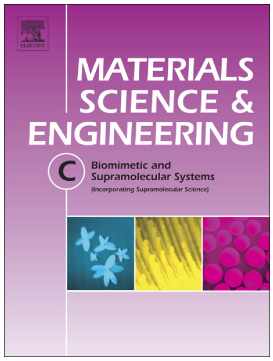

Electrophoretic deposition of organic/inorganic composite coatings containing ZnO nanoparticles exhibiting antibacterial properties

Joanna Karbowniczek, Luis Cordero-Arias, Sanna Virtanen, Superb K. Misra, Eugenia Valsami-Jones, Bogdan Rutkowski, Kamil Górecki, Piotr Bała, Aleksandra Czyrska-Filemonowicz, Aldo R. Boccaccini

PII: S0928-4931(16)31310-8
DOI: doi: 10.1016/j.msec.2017.03.180
Reference: MSC 7692

To appear in: *Materials Science & Engineering C*

Received date: 13 September 2016
Revised date: 22 January 2017
Accepted date: 21 March 2017

Please cite this article as: Joanna Karbowniczek, Luis Cordero-Arias, Sanna Virtanen, Superb K. Misra, Eugenia Valsami-Jones, Bogdan Rutkowski, Kamil Górecki, Piotr Bała, Aleksandra Czyrska-Filemonowicz, Aldo R. Boccaccini , Electrophoretic deposition of organic/inorganic composite coatings containing ZnO nanoparticles exhibiting antibacterial properties. The address for the corresponding author was captured as affiliation for all authors. Please check if appropriate. Msc(2017), doi: 10.1016/j.msec.2017.03.180

This is a PDF file of an unedited manuscript that has been accepted for publication. As a service to our customers we are providing this early version of the manuscript. The manuscript will undergo copyediting, typesetting, and review of the resulting proof before it is published in its final form. Please note that during the production process errors may be discovered which could affect the content, and all legal disclaimers that apply to the journal pertain.

ACCEPTED MANUSCRIPT

Electrophoretic deposition of organic/inorganic composite coatings containing ZnO nanoparticles exhibitiong antibacterial properties

Joanna Karbowniczek[a], Luis Cordero-Arias[b,c], Sanna Virtanen[d], Superb K. Misra[e], Eugenia Valsami-Jones[f], Bogdan Rutkowski[a], Kamil Górecki[a], Piotr Bała[a,g] Aleksandra Czyrska-Filemonowicz[a], Aldo R. Boccaccini[b*]

[a] Faculty of Metals Engineering and Industrial Computer Science, AGH University of Science and Technology, Al. A. Mickiewicza 30, PL-30059 Krakow, Poland

[b] Institute of Biomaterials, Department of Materials Science and Engineering, University of Erlangen-Nuremberg, Cauerstrasse 6, D-91058 Erlangen, Germany

[c] Escuela de Ciencia e Ingeniería de los Materiales (ECIM), Costa Rican Institute of Technology (ITCR), Cartago 159-7050, Costa Rica

[d] Institute for Surface Science and Corrosion, Department of Materials Science and Engineering, University of Erlangen-Nuremberg, Martensstrasse 7, D-91058 Erlangen, Germany

[e]Materials Science and Engineering, Indian Institute of Technology-Gandhinagar, India

[f] School of Geography, Earth and Environmental Sciences, University of Birmingham, Edgbaston, Birmingham, B15 2TT, UK

[g] Academic Centre for Materials and Nanotechnology, AGH University of Science and Technology, Al. A. Mickiewicza 30, PL-30059 Krakow, Poland

*corresponding author: aldo.boccaccini@ww.uni-erlangen.de

Abstract

To address one of the serious problems associated with permanent implants, namely bacterial infections, novel organic/inorganic coatings containing zinc oxide nanoparticles (nZnO) are proposed. Coatings were obtained by electrophoretic deposition (EPD) on stainless steel 316L. Different deposition conditions namely: deposition times in the range 60-300 s and applied voltage in the range 5-30 V as well as developing a layered coating approach were studied. Antibacterial tests against gram-negative *Staphylococcus aureus* and gram-positive *Salmonella enteric* bacteria confirmed the activity of nZnO to prevent bacterial growth. Coatings composition and morphology were analyzed by thermogravimetric analysis, Fourier transform infrared spectroscopy, scanning electron microscopy and energy dispersive X-ray spectroscopy. Moreover, the corrosion resistance was analyzed by evaluation of the polarization curves in DMEM at 37°C, and it was found that coatings containing nZnO increased the corrosion resistance compared to the bare substrate. Considering all results, the newly developed coatings represent a suitable alternative for the surface modification of metallic implants.

ACCEPTED MANUSCRIPT

Keywords: Antibacterial surfaces; coatings; electrophoretic deposition; ZnO nanoparticles; chitosan; bioactive glass

1. Introduction

In the area of orthopedic and dental implants, designed for long-term use, increasing attention is being dedicated to the durability of such biomaterials [1, 2]. Scientific research and development are mainly aimed at increasing the surface biocompatibility. To replace hard tissues metals (titanium alloys, cobalt-chromium alloys or stainless steel) are the materials of choice, because of their superior mechanical properties, corrosion and wear resistance as well as biotolerance [2–4]. However, a factor that may lead to implant failure is surgery related infection. Complications caused by infections occur in the 1-2 % of total hip replacements procedures [5, 6]. The increasing number of joint replacements being performed means that the absolute number of such infections is significant, increasingly posing substantial costs to the healthcare system [5]. The most common pathogen following orthopedic procedures is *Staphylococcus aureus* [5, 6]. Therefore, the demand for biomaterials with antibacterial properties is increasing [7, 8].

Surface modifications, including coatings on metallic biomaterials represent a common approach to improve biocompatibility and bioactivity or to create antibacterial or drug releasing surfaces while preserving the bulk material properties [1]. Different methods might be applied to obtain antibacterial surfaces. One approach is the loading of the surface of the biomaterial with antibiotics. Vancomycin might be incorporated into the porous structure of ceramic coatings or loaded to sol-gel thin films by simple immersion of the material in antibiotic solutions [9, 10] or covalently bonded to the oxidized surface of Ti6Al4V alloy substrate [11]. Another approach is the co-deposition of silver as an antimicrobial agent by different methods. For example silver containing ceramic coating deposited on commercially pure titanium (Cp-Ti) alloy by micro-arc oxidation [12], silver containing hydroxyapatite coating deposited on Cp-Ti by magnetron sputtering [13], Ag-SiO_2 thin film formed on glass substrate by sol-gel method [5], titanium/silver coating deposited on Cp-Ti by physical vapor deposition (PVD) [15], bioactive glass/ chitosan/ nano-silver coating deposited on 316L stainless steel by electrophoretic deposition (EPD) [16] and Zn-doped BG/chitosan coatings [17], among others.

EPD is a fast and efficient method to produce organic/inorganic coatings on metallic substrates [18]. With simple adjustment of the applied potential, deposition time and suspension composition it is possible to control the thickness and microstructure of the deposited films [19]. EPD offers many possibilities in terms of surface modifications of metallic materials for medical applications. For example, bioactivity may be achieved by depositing hydroxyapatite or bioactive glass (BG) containing

ACCEPTED MANUSCRIPT

coatings [18-22]. For the materials that have a direct contact with blood the anti-thrombogenic property is very important to prevent blood clot formation. In such application, composite heparin containing coating might be deposited, creating anti-thrombogenic surfaces [23]. Moreover, it is also possible to produce antibacterial films with nano-silver, zinc oxide (ZnO) nanoparticles or BG by EPD [18, 24, 25].

Zinc oxide is described as a versatile inorganic material with a broad range of applications. In the form of nanoparticles (nZnO), it has antimicrobial activity against both Gram-positive (G+) and Gram-negative (G-) bacteria [26, 27]. The exact mechanism of the antimicrobial activity of ZnO continues to attract the interest of researchers. One of the theories put forward suggests that reactive oxygen species (ROS) that are produced by nZnO in aqueous suspensions cause the destruction of cellular components such as proteins, lipids and DNA of bacterial cells. Another toxicity mechanism might be based on zinc ions (Zn^{2+}) release. Those ions have a significant effect in the active transport inhibition as well as in the amino acid metabolism and enzymes system disruption [28]. In general the antibacterial properties of nanomaterials are enhanced by their high specific surface to volume ratio [27, 28].

The antimicrobial properties of nZnO are well established, however there has been only limited research work investigating the effect of a polymer matrix embedding nZnO on the antibacterial activity of the particles, which is the case of functional coatings for medical applications. The incorporation of nZnO into polymer matrices or films is frequently studied in the context of food packaging. Silvestre et al. [29] for example showed the antibacterial effect of composite films based on isostatic polypropylene with nZnO on *E. Coli.* Venkatesan et al. [30] studied the antibacterial activity of poly(butylene adipate-co-terephthalate) loaded with nZnO. Regarding medical applications, Seil et al. [31] observed reduced growth of *S. Aureus* after incubation with polyvinyl chloride incorporated with nZnO.

The aim of the present research was to develop and characterize complex organic/inorganic coatings with antibacterial activity produced by EPD on stainless steel 316L substrate. As an antimicrobial agent nZnO was chosen and combined with sodium alginate and polyvinyl alcohol matrix to develop “soft” antibacterial coatings intended for orthopedic applications. Additionally bioactive glass was added to improve the bioactivity of the coating. Moreover, a multilayer approach was proposed using chitosan interlayers, in order produced robust, multicomponent coatings.

ACCEPTED MANUSCRIPT

2. Materials and methods

Zinc oxide nanoparticles (Intrinsiq Materials, UK) and bioactive glass microparticles (5-25 µm particle size) of 45S5 composition [32] were used as inorganic fillers. Sodium alginate (Alg; Sigma Aldrich, Germany), polyvinyl alcohol (PVA; MW 30.000, degree of hydrolysis ≥ 98%, VRW) and chitosan (Ch; 80kDa, 85% deacetilation, Sigma) were employed for the organic part (matrix) of the coatings. Pure water (Purelas option ELGA DV25 0.67 µS/cm) and ethanol (99.5% with 1% methyl ethyl ketone, Emsure) were used as solvents.

Four different types of coatings were studied: (a) nZnO/Alg-PVA (nZAP) and (b) nZnO-BG/Alg-PVA (nZBAP); and using a multilayer approach: (c) nZnO/Alg-PVA//Ch (nZAPC) and (d) nZnO-BG/Alg-PVA//Ch (nZBAPC). To help to visualize the expected structure of the different coatings, schematic diagrams are presented in Figure 1.

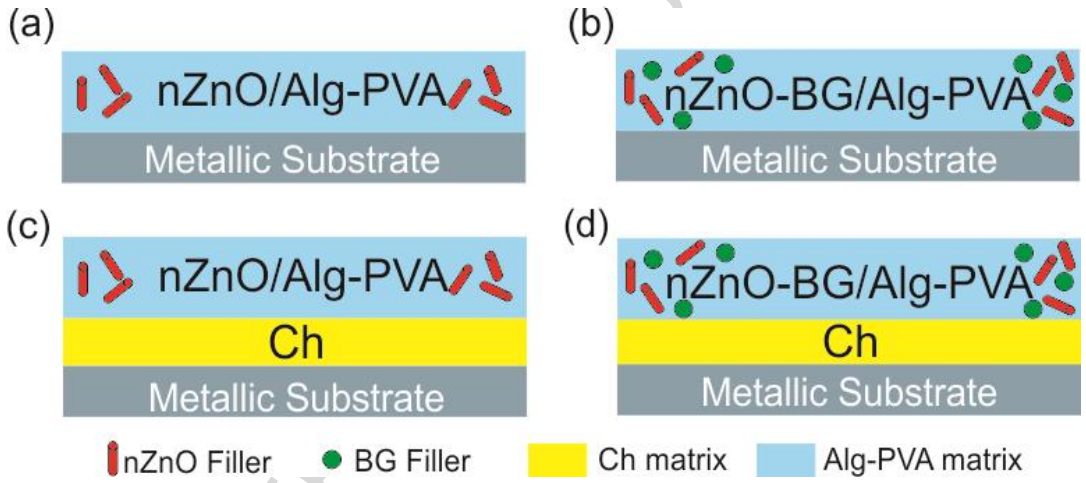

Fig. 1 Schematic representation of the different coatings studied: nZAP (a), nZBAP (b), nZAPC (c), nZBAPC (d).

In order to avoid hydrogen evolution formation during the EPD process (due to water electrolysis) a mixture of 40 vol.% ethanol – 60 vol.% water was used [33, 34] to produce the suspension containing alginate (0.5g/L) and PVA (5g/L). For the production of this suspension PVA was dissolved in water at 80°C. After this, the solution was cooled to room temperature and Alg was added. When Alg was totally dissolved ethanol was added. Subsequently, the ceramic fillers were added giving a final amount of 2.5g/L (100wt.% nZnO for the nZAP coating and a mixture 50wt.% nZnO /50wt.% BG for the nZBAP coating). When chitosan was used the solution was produced using 79 vol.% ethanol, 20 vol.% water and 1 vol.% acetic-acid (Sigma-Aldrich) [34]. The addition of acetic acid was required to dissolve the chitosan [35, 36]. The chitosan layer was deposited from a solution containing 0.5g/L of

ACCEPTED MANUSCRIPT

Ch. As deposition conditions for this layer, 1 min of deposition time and 25 V as potential were employed [7].

To achieve an adequate dispersion of the components, the suspensions were magnetically stirred for 10 min followed by 30 min of ultrasonication (using an ultrasonic bath, Bandelin Sonorex, Germany). Colloidal stability of the suspensions was analysed using zeta-potential measurements. These measurements were done by the Laser Doppler Velocimetry (LDV) technique using a Zetasizer nano ZS equipment (Malvern Instruments, UK). The solid content of all suspensions was adjusted to 0.1 g/L in order to ensure reliable measurements.

Constant voltage EPD (DC-EPD) was used to deposit the coatings on stainless steel AISI 316L (Thyssenkrupp) electrodes. The surface of electrodes was ultrasonically cleaned in ethanol for 15 minutes and air dried prior to deposition. The distance between the electrodes in the EPD cell was kept constant at 10 mm. Deposition voltages and times in the ranges 5-30 V and 60-300 s, respectively, were studied. The deposition yield was evaluated using an analytical balance (precision 0.0001g). Coated substrates were dried during 24 h in normal air at room temperature prior to mass determination.

In order to characterize the coatings, Fourier transform infrared spectroscopy (FTIR) (Bruker Instruments, Germany) and thermogravimetric (TG) analysis (SDT Q600, TA INSTRUMENTS) in air (heating rate: 10°C/min) were performed. The microstructure of the ZnO nanoparticles was characterized by transmission electron microscopy (TEM) (Tecnai G2 20 TWIN, FEI) and selected area electron diffraction (SAED); obtained patterns were interpreted with Java Electron Microscopy Software (JEMS) [37]. The surface microstructure and composition of the coatings were analyzed by Scanning electron microscopy (SEM) Merlin Gemini II (ZEISS) and energy-dispersive X-ray spectroscopy (EDS), respectively.

The electrochemical behavior of the coatings was studied in order to test their possible corrosion protective properties. Potentiodynamic polarization curves were obtained using a potentiostat/galvanostat (Autolab PGSTAT 30). The samples were immersed in 50 mL of Dulbecco´s MEM (DMEM, Biochrom) at 37°C. A conventional three electrode system was used, where a platinum foil served as counter electrode and Ag/AgCl (3M KCl) was used as reference electrode. The analysis was carried out using an O-ring cell with an exposed sample area of 0.38 cm^2 with a potential sweep rate of 1 mV/s.

The bioactivity of the coatings was determined through immersion in simulated body fluid (SBF) using Kokubo's protocol [38]. The samples with an area of 2.25 cm^2 were immersed in 40 mL SBF

ACCEPTED MANUSCRIPT

(pH = 7.4) during 2, 5, 8, 14 and 22 days at 37°C. SEM-EDS was used to evaluate the formation of hydroxyapatite (HA) on the coatings.

The antibacterial activity of all samples was investigated against the gram-negative *Staphylococcus aureus* (*S. aureus, strain:* LS1) and gram-positive *Salmonella enterica (S. enterica,* strain ArJEG) using the method described in literature [39, 40]. Prior to the test all samples were disinfected through washing for 5 min in 70 % ethanol. *S. aureus* and *S. enterica* were grown in trypic soy broth (TBS) to a concentration 5 x 10^7 colony forming units (CFU). 5 ml of bacterial suspension was transferred onto the samples and incubated for 1 hour at room temperature. Afterwards samples were rinsed in PBS to remove unbound bacterial cells. Subsequently samples were transferred to sterile falcon tubes and rinsed in 5 ml of PBS, the tubes were vortexed and sonicated for 15 minutes to release attached cells. Samples were removed and the remaining suspension was plated and cultured at 37°C for 48 hours. The number of viable adherent bacteria was calculated.

3. Results and discussion

3.1 Zinc oxide nanoparticles characterization

The as-received nZnO particles were analyzed by means of SEM and TEM (Fig. 2) to determine their size, shape and purity. Observed particles could be categorized into 3 groups: majority of elongated hexagonal shape with average length of 215 nm, few large particles with rectangular parallelepiped shape and average dimensions of 378x140x100 nm, and circular shape particles with average diameter of 40,8 nm. Based on measurements of particles dimensions the specific surface area was estimated to be in the range of 15-20 m^2/g (assuming ideal geometrical shapes of the particles). In the SEM-EDS spectra (Fig. 2 c) the main components are zinc and oxygen confirming homogenous composition of the nanoparticles, carbon is the typical contamination element and alumina peak comes from the specimen stub used for the measurement. Phase analysis using SAED was performed not on single particle but on a larger area containing a large amount of particles. Due to random orientation of crystals on the carbon substrate, a ring pattern was formed. It was identified by JEMS software as ZnO (Fig. 2 d).

ACCEPTED MANUSCRIPT

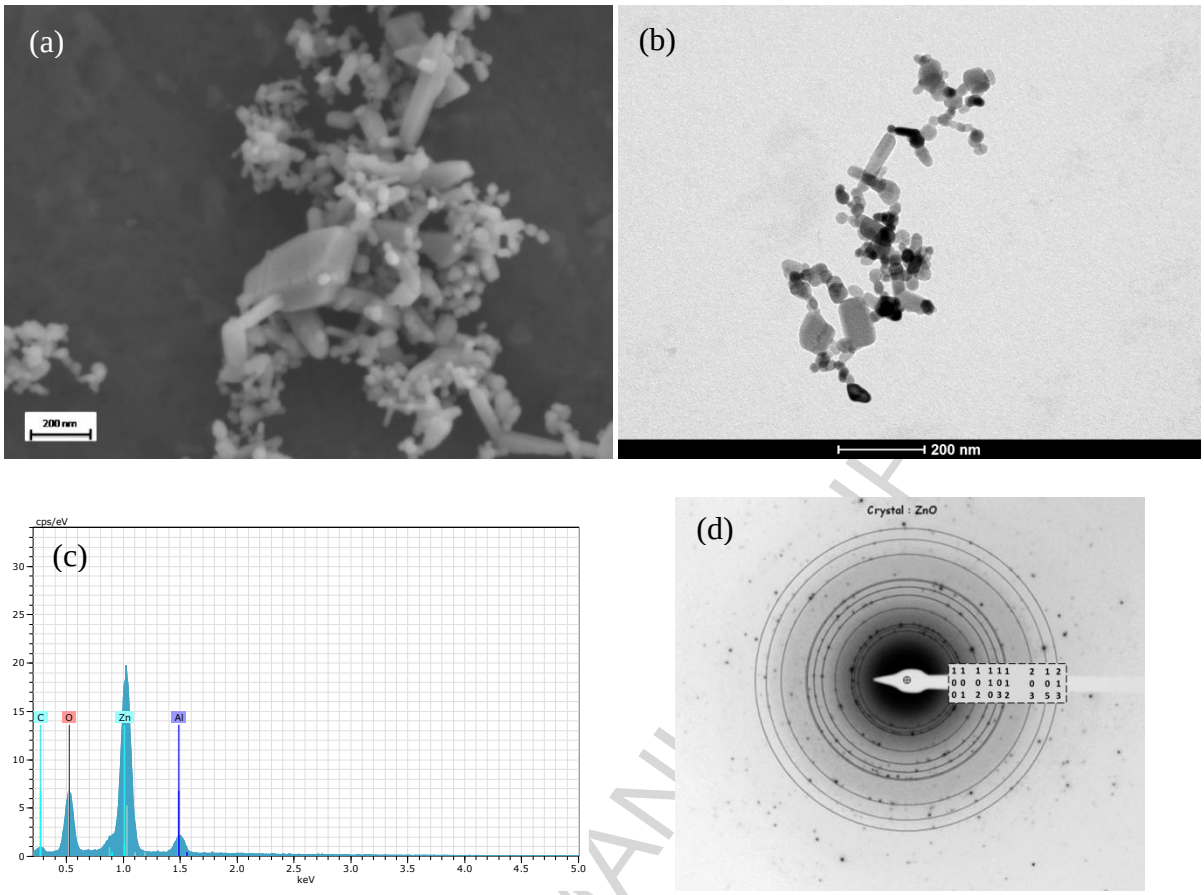

Fig.2. ZnO nanopraticles: SEM image (a), TEM image (b), SEM-EDS spectra (c), SAED pattern (d).

3.2 Stability of the suspensions for EPD

The zeta potential values for different suspensions are presented in Table 1. The zeta potential gives information about the stability of the colloidal dispersion by indicating the degree of electrostatic repulsion between adjacent charged particles in suspension. Low values of zeta potential mean that attractive forces between particles exceed the repulsion forces and the dispersion tends to coagulate or flocculate. It is well-known that high zeta potential values (negative or positive) are characteristic for electrically stabilized colloids [19]. Zeta potential values for different suspensions are presented in Table 1. Low positive zeta potential values for nZnO suspension indicate the presence of positive charges on the particles surface as well as instability of the system and tendency to coagulate. In case of the BG suspension the negative value of zeta potential (-22,6 ± 1,9) is caused by the predominant presence of silanol groups ($SiOH^-$) on the surface of bioactive glass particles [41]. Possible solution to improve the stability of the suspension against flocculation is the modification of the particles' surface by polymer adsorption [42]. For charged polymer-adsorbent systems mainly strong electrostatic interactions are present, while for uncharged polymers only hydrogen bridges and solvation interactions are important [43]. Thus sodium alginate (Na-Alg) was added to nZnO and BG

ACCEPTED MANUSCRIPT

suspensions. In water solutions Na-Alg undergoes dissociation and anionic Alg^- species are formed [20, 34]. Alg^- reacts via electrostatic interactions with positively charged ZnO particles and stabilizes the system, thus high negative values of zeta potential were measured. Addition of sodium alginate to the BG suspension caused an increase of the absolute value of zeta potential. This behavior can be explained by electrostatic interactions between Alg^- and positive charges at the BG particle surface [44]. After adding PVA to colloidal suspensions containing Alg and ceramic particles (ZnO and/or BG), a decrease of the absolute values of zeta potential was observed, which is consistent with findings previously described in the literature [45]. Polyvinyl alcohol is classified as a nonionic polymer, however it contains hydroxyl groups (-OH) and some nonhydrolysed acetate groups ($-OCOCH_3$) [40, 45]. The decrease in zeta potential in the presence of PVA can be caused by the shift of the slipping plane due to polymer adsorption or the presence of functional groups [45]. Based on the zeta potential values and chemical structure of the molecules possible schematic representation of the interactions between compounds used in the nZnO-BG/Alg-PVA suspension is presented in Fig. 3.

Table 1

Zeta potential values for different suspension compositions investigated in this study.

Suspension	**Zeta-potential (mV)**
nZnO	6.9 ±0.2
BG	-22.6 ± 1.9
nZnO-BG	-19.6 ± 2.5
nZnO/Alg	-47.9 ±1.1
BG/Alg	-44.7 ±3
nZnO-BG/Alg	-52.5 ±0.5
nZnO/ Alg-PVA	-32.7 ± 0.4
BG/ Alg-PVA	-42.1 ± 0.8
nZnO-BG/Alg-PVA	-35.8 ± 1.6

ACCEPTED MANUSCRIPT

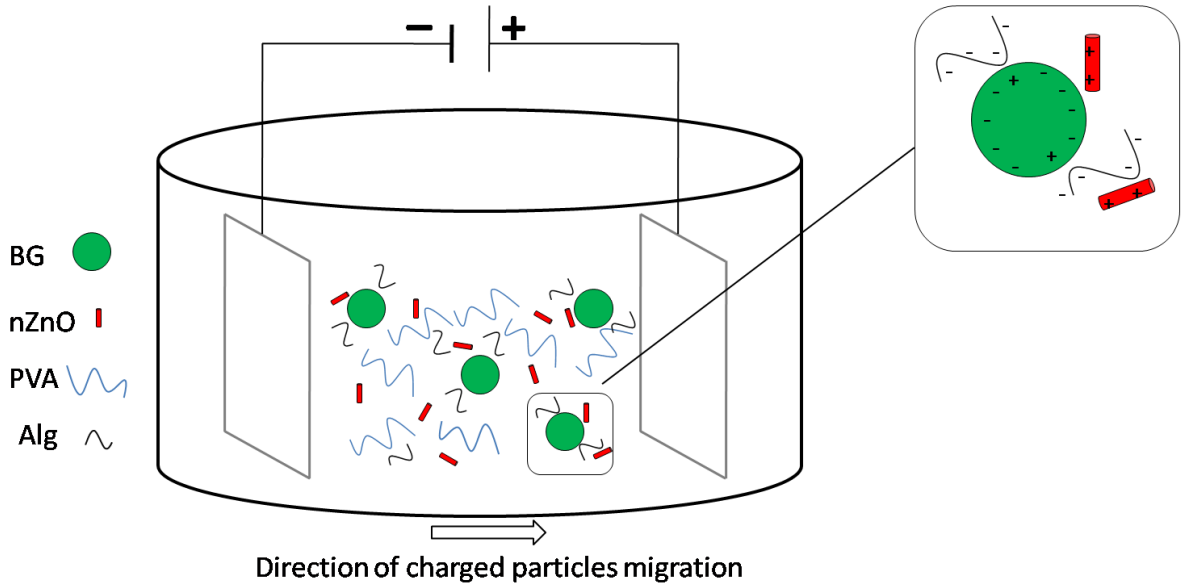

Fig. 3. Schematic representation of the interactions between the compounds used in the suspension for obtaining nZnO-BG/Alg-PVA coatings by EPD

3.3 Electrophoretic deposition and coatings characterization

To adjust the EPD process parameters a series of coatings were deposited with applied potentials in the range 5-30 V and deposition time between 60 and 300 seconds. Two main suspension compositions were used: nZAP (5g/L of PVA, 0,5gL of Alg, 2,5g/L of nZnO) and nZBAP (5g/L of PVA, 0,5gL of Alg, 1,25g/L of nZnO , 1,25g/L of BG), with or without chitosan interlayer. The deposition yield of four configurations of prepared coatings versus applied voltage is presented in Fig. 3, in all cases the reaction time was set to 1 minute. For all types of investigated samples the increase of applied voltage resulted in higher deposition yield. Moreover, it was observed that with functionalization of the stainless steel substrate with an interlayer of chitosan higher deposition yield was obtained. Based on macro and microscopic observations as well as on the results of bending test, two types of samples, namely nZAPC and nZBAPC, both deposited using 20 V and 1 min with chitosan interlayer, were selected for further investigation. In both proposed systems the stainless steel substrate was homogenously covered by an organic/inorganic coatings, with uniform distribution of the ceramic particles embedded in the polymer matrix and exhibiting crack-free microstructure, as confirmed by light microscopy images (Fig. 4) for nZAPC and nZBAPC coatings.

ACCEPTED MANUSCRIPT

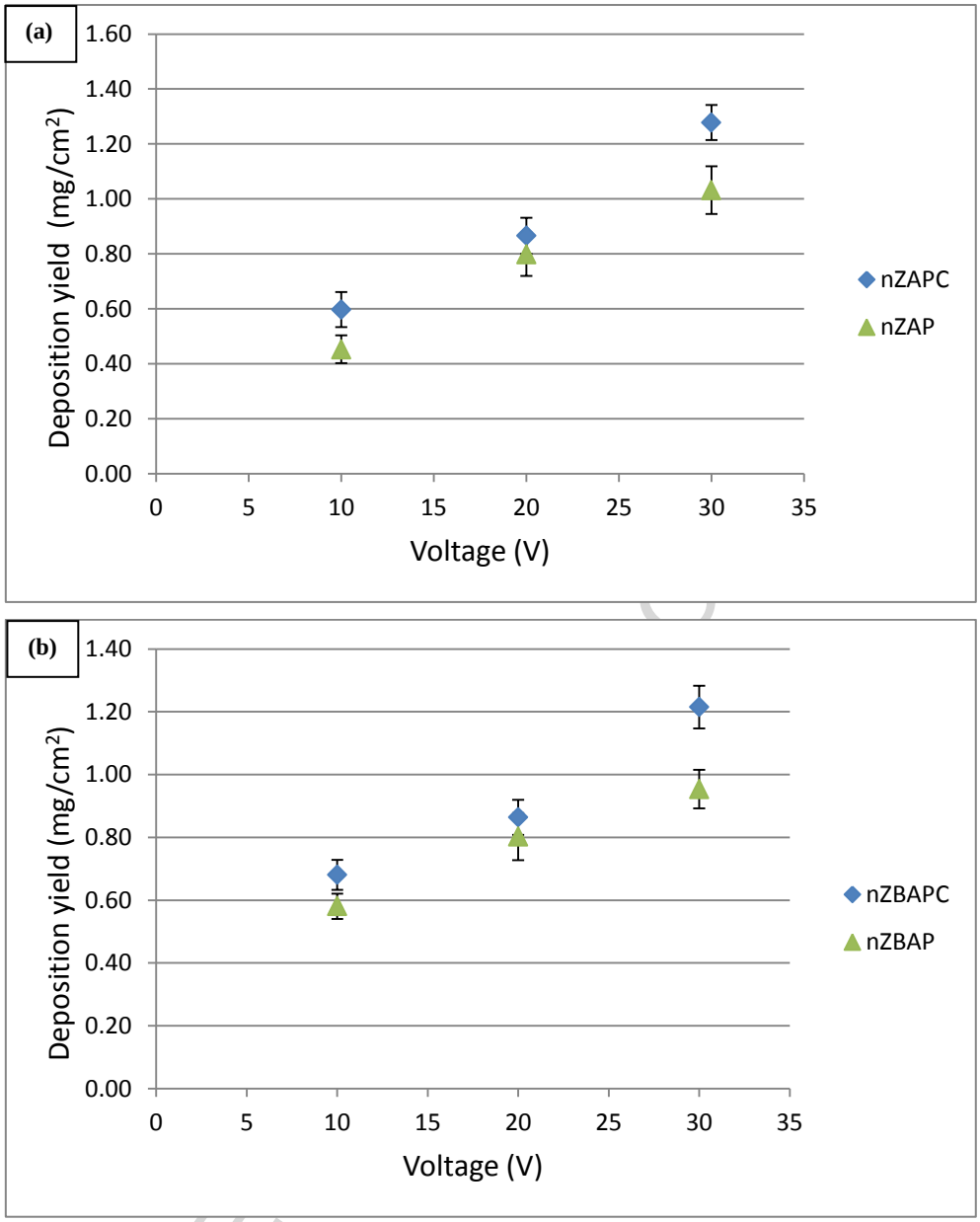

Fig. 3.Calculated deposition yield for different suspensioncompositions: nZAP with and without interlayer of chitosan (a), nZBAP with and without interlayer of chitosan (b).

ACCEPTED MANUSCRIPT

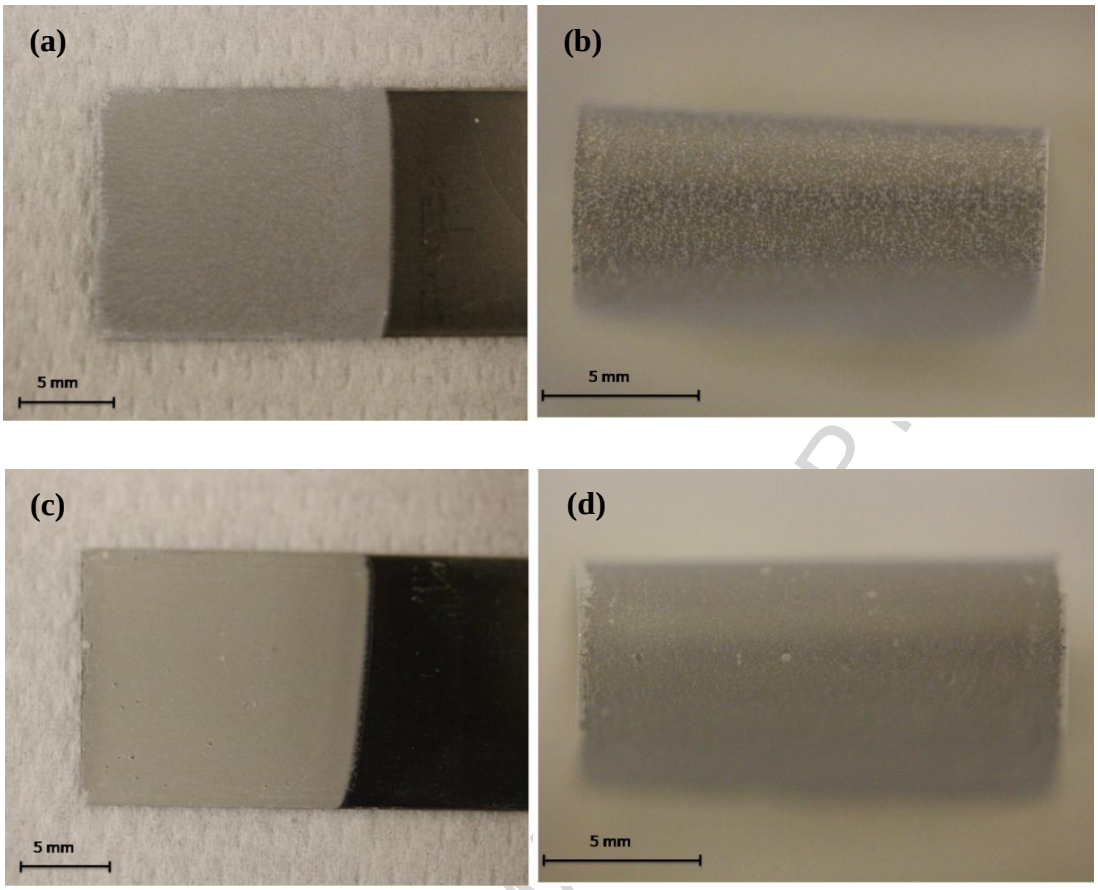

Fig. 4. Images of coatings deposited on 316L stainless steel substrate: nZAPC (a), nZBAPC (c); surface of the coatings after the qualitative banding test: nZAPC (b), nZBAPC (d).

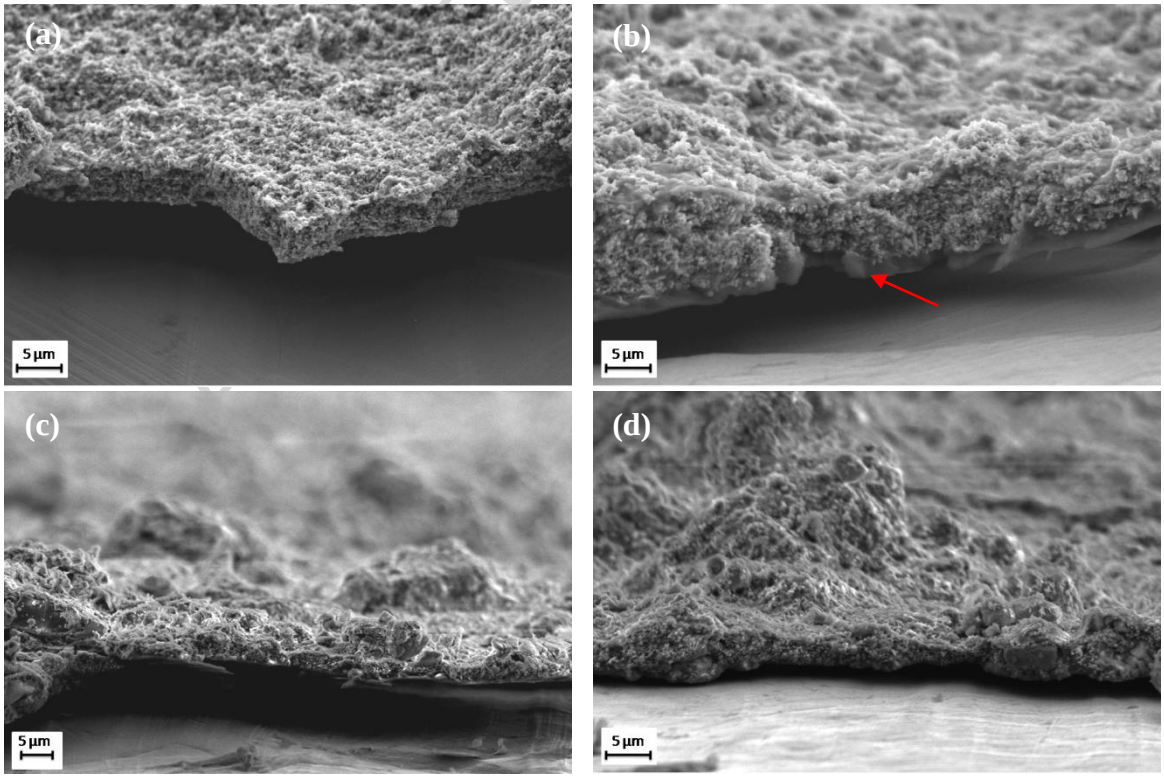

ACCEPTED MANUSCRIPT

Fig. 5. Cross-sections of four studied coatings: nZAP (a), nZAPC with Ch interlayer marked by red arrow (b), nZBAP (c), nZBAPC (d).

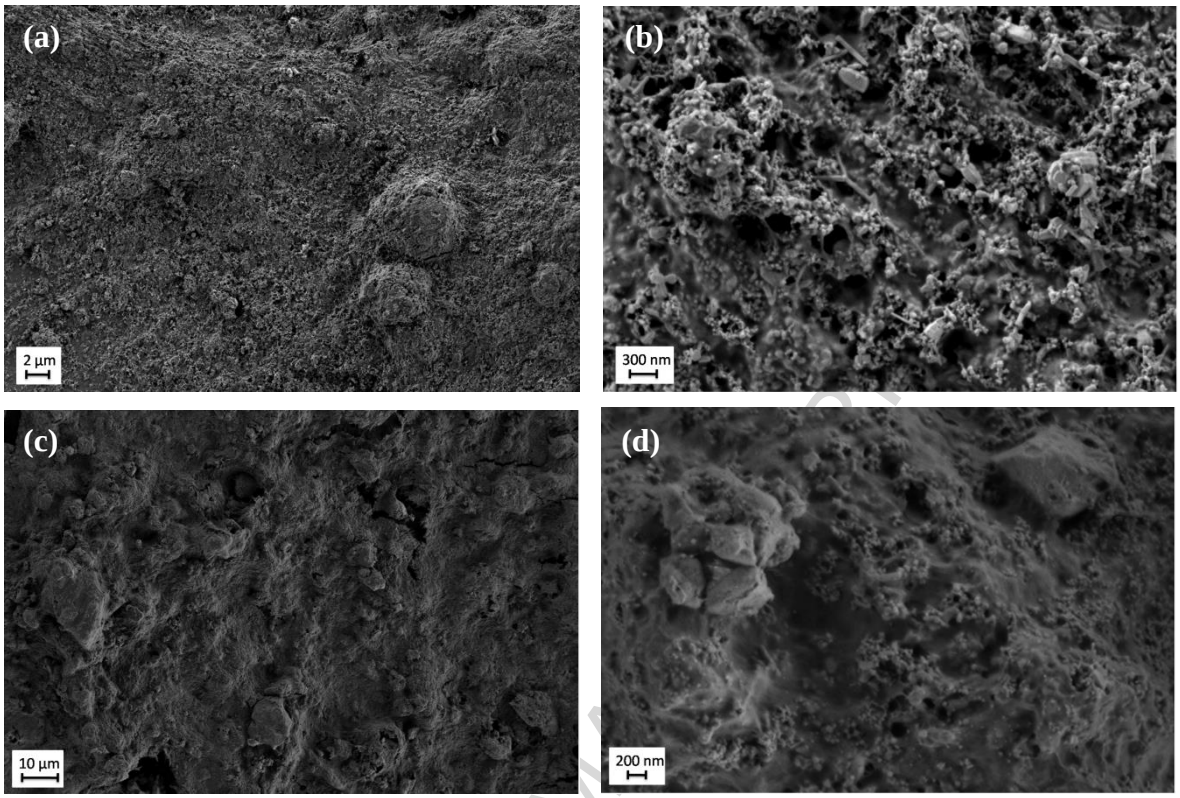

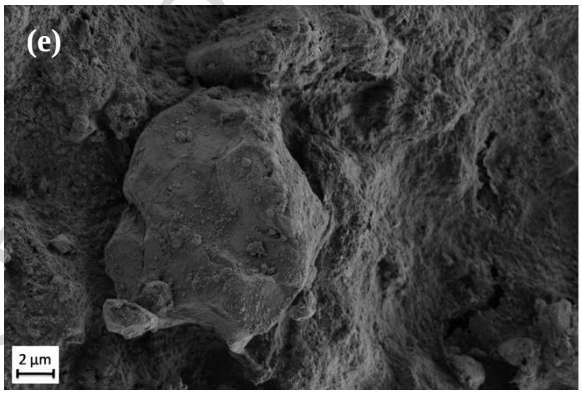

Fig. 6. SEM images of deposited coatings: low and high magnification of nZAPC coating (a) and (b) respectively, low and high magnification of nZBAPC coating (c) and (d), respectively, as well as SEM micrograph of a bioactive glass particle present in the polymer coating (e).

The cross-section images of the four studied coatings are presented in Fig. 5. A high amount of nZnO particles is present throughout the coatings thickness. Coatings with Ch interlayer exhibited a polymer layer without any incorporated particles as the first layer on the substrate, see Fig. 5b. Completing the coatings' characterization, Fig. 6 (a-e) show typical SEM images of deposited coatings (nZAP and nZBAP) at different magnifications while Fig. 7 shows the FTIR results for both nZAP and

ACCEPTED MANUSCRIPT

nZBAP coatings, as well for alginate, PVA, BG and n-ZnO powders. The presence of alginate in both coatings was confirmed by the characteristic peaks of both the asymmetric and the symmetric stretching of COO^- group at 1623 cm^{-1} and 1415 cm^{-1}, respectively [46]. The PVA spectrum exhibits the characteristic bonds corresponding to the vibration of C-H (2944, 2904 and 854 cm^{-1}) and C-O (1143 cm^{-1}) bands [44, 47, 48]. The BG powder spectrum shows the characteristic asymmetric stretching and bending peaks of the Si-O-Si bonds at ~1035, 924 and 500 cm^{-1} [33, 34, 43, 44], respectively, confirming the presence of BG in the nZBAP coating. The peak at 1384 cm^{-1} present in the ZnO powder as well as in nZAP and nZBAP coating spectrum corresponds to the symmetrical stretching of the zinc carboxylate, which is a frequent impurity in ZnO nanoparticles [51].

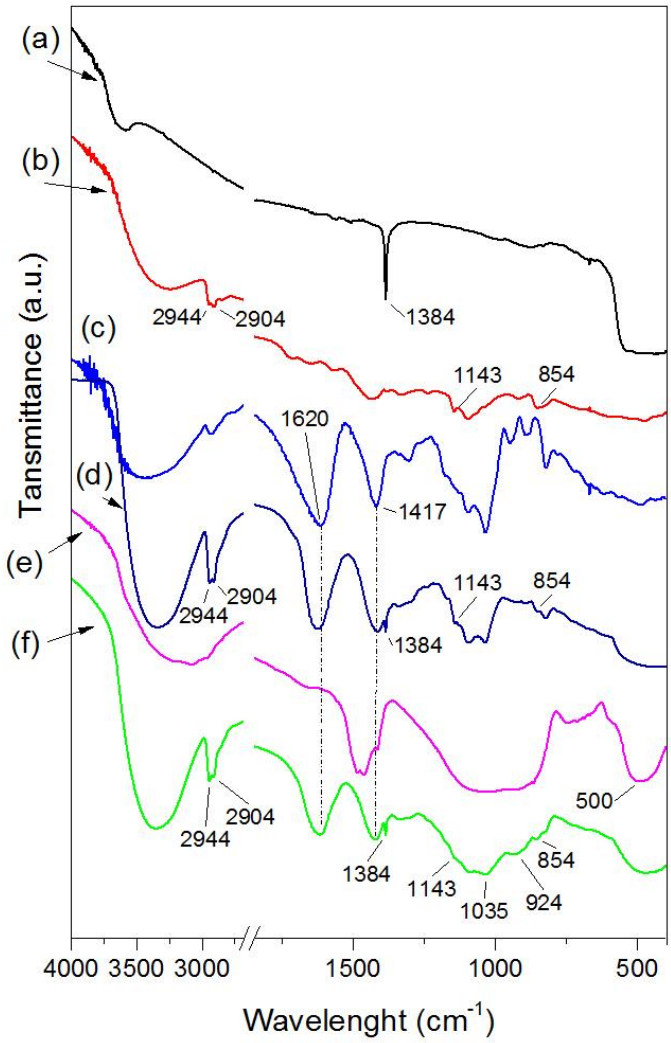

Fig. 7. FTIR results of the different coatings and their components: nZnO (a), PVA (b), Alg (c), nZnO/Alg-PVA (d), BG (e), nZnO-BG/ Alg-PVA (f). (The relevant peaks are explained in the text).

Thermogravimetric curves of deposited coatings are presented in Fig.8. For both samples (nZAP and nZBAP) three well separated mass losses are observed. First, the mass loss in the interval 50-100 °C is

ACCEPTED MANUSCRIPT

attributed to the removal of absorbed water [25, 34, 44]. Subsequently, in the temperature range 220-280 °C burning out of alginate and dehydroxylation of PVA takes place. The third mass loss in the temperature range 380-480 °C is attributed to the final decomposition of PVA molecules. Above 500 °C no significant mass loss was recorded, thus this temperature was selected to determine the residual inorganic phase content: in sample nZAP this value was 58 wt%, while for sample nZBAP it was 55 wt%. Table 2 presents the final compositions of both coatings.

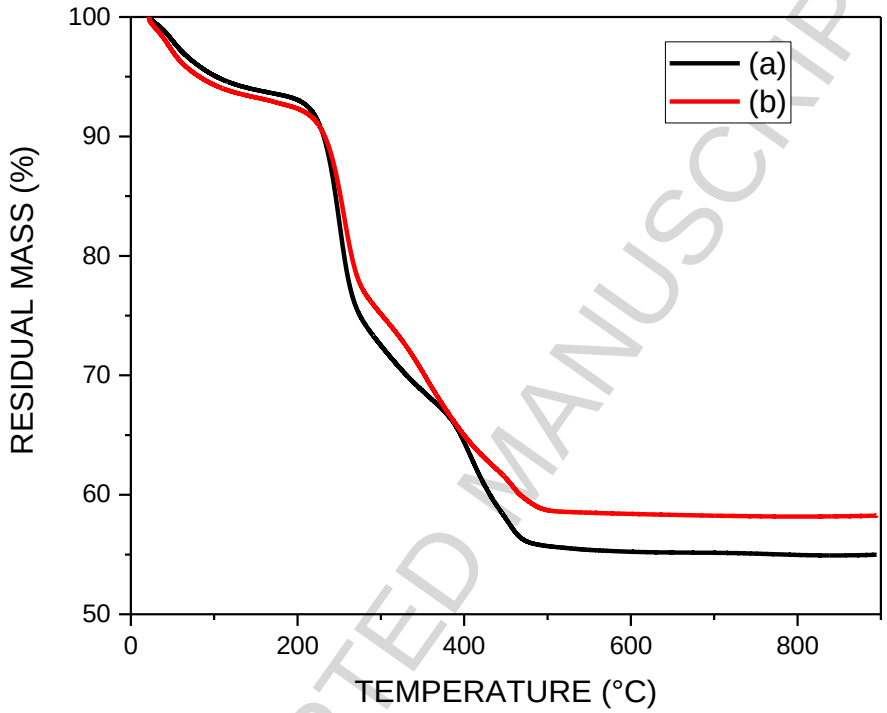

Fig.8. Theromgravimetric curves of deposited coatings: nZBAP (a), nZAP (b).

Table 2. Final composition of the coatings nZAP and nZBAP based on the TG/DTA analysis.

Sample	Final concentrations of the components in the coatings		
	Water (wt%)	Alginate and PVA (wt%)	Inorganic phase (wt%)
nZAP	6	40	55 (nZnO)
nZBAP	5	36	58 (nZnO + BG)

3.4 Corrosion resistance

The electrochemical behavior of implanted metallic biomaterial in the human body is a crucial parameter determining implant functionality and safety. Corrosion and surfaces oxide film dissolution might be on one hand deleterious for adjacent tissues and on the other hand may lead to

ACCEPTED MANUSCRIPT

mechanical failure of the medical device [49]. Potentiodynamic polarization curves of untreated 316L stainless steel substrate as well as different compositions of prepared coated samples are presented in Fig. 9. The corrosion potential and corrosion density current values were determined from the polarization curves and results are shown in Table 3. Compared with the bare substrate a chitosan coating increases considerably the corrosion potential, it denotes a reduction of the corrosion tendency of the system. The corrosion current density is also reduced, meaning a lower corrosion velocity, which is mainly due to the barrier effect of a homogenous chitosan layer that inhibits the direct contact of the medium and the metallic surface. In the case of the nZAP and nZAPC coatings, an increase of the corrosion potential (tendency) is observed for both coatings compared with the bare sample. It can be observed that the electrochemical behavior of both coatings is quite similar. This means that the additional chitosan layer in the nZAPC coating did not induce any change in terms of electrochemical behavior. This could imply a possible reaction of the chitosan with the nZnO/Alg-PVA layer, or possible damage of this first layer during the deposition of the second layer. In terms of corrosion velocity both systems, namely nZAP and nZAPC, presented a similar behavior as the bare steel sample. This means that these coatings did not affect the reaction kinetics of the metal, but they provide a layer with possible antibacterial properties and the presence of a polymer that is obviously much more similar to the extracellular matrix than the metal. In case of both coatings containing bioactive glass particles, nZBAP and nZBAPC, the one containing the chitosan layer shows a slightly increment of the corrosion potential, but both of them show a lower stability and higher corrosion rate than the bare substrate, what could be related to the presence of BG. As previously reported [25], bioactive glass particles undergo dissolution in DMEM, thus increasing the activity of the whole system exposing the metallic surface to the liquid. In the case of both prepared coatings, nZBAP and nZBAPC, there was no protection of the stainless steel substrate against corrosion. On the other hand the positive effect of BG particles must be considered, as they have the potential to contribute to bone formation around the metallic implant [xx]. Furthermore, at high polarization potentials (up ≈-400 mV), all coated samples presented a shift of the anodic arm to much lower current densities compared with the bare 316L sample and the chitosan coated sample, this phenomenon could be related to the barrier effect of the coating and the possible increment of the pH adjacent to the sample, due to the alginate dissolution in the medium.

ACCEPTED MANUSCRIPT

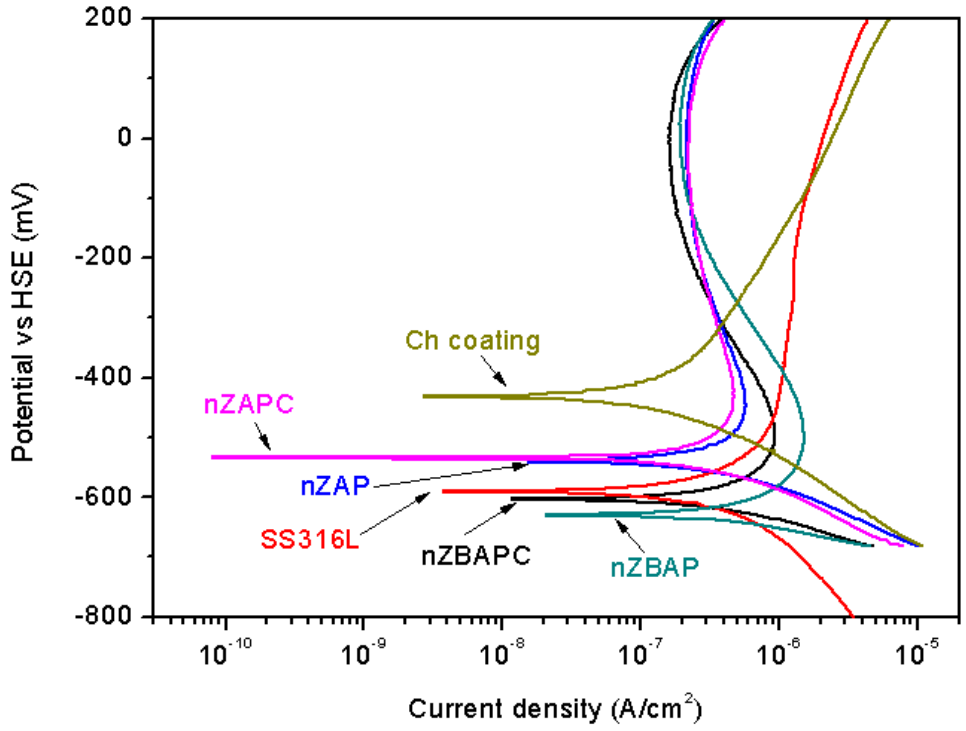

Fig. 9. Polarization curves for bare 316L stainless steel, chitosan coated 316L substrate, nZAP coating, nZBAP coating, nZAPC coating and nZBAPC coating, measured in Dulbecco's MEM at 37°C

Table 3. Corrosion potential and current density for the stainless steel AISI 316L bare sample and different coated samples derived from the polarization curves (Fig. 9)

Sample	Corrosion Potential (mV)	Corrosion Current Density (A/cm^2)
SS316L	-589	$2.29x10^{-7}$
Ch coating	-430	$9.04x10^{-8}$
nZAP	-552	$2.61x10^{-7}$
nZBAP	-640	$4.78x10^{-7}$
nZAPC	-531	$2.33x10^{-7}$
nZBAPC	-607	$4.24x10^{-7}$

3.5 *In vitro* bioactivity

Bioactive glass particles are known to promote hydroxyapatite precipitation while incubated in SBF [20, 25, 34]. This hydroxyapatite formation is considered to enhance the bone bonding ability of the biomaterial [8]. To evaluate possible bioactive properties of the prepared organic/inorganic coatings, samples were immersed in SBF at 37 °C up to 22 days and subsequently analyzed by SEM-EDS. The first evidence of calcium phosphates deposition at the nZBAPC surface was found after 2 days of incubation (Fig. 10). With longer incubation time the amount of calcium phosphate increased. For

ACCEPTED MANUSCRIPT

samples without BG particles, containing only nZnO in polymer matrix (nZAPC), some minor evidence of calcium phosphate precipitation was observed after 14 and 22 days of incubation in SBF (data not shown). However, significantly less amount of CaP precipitated than in the case of samples containing BG.

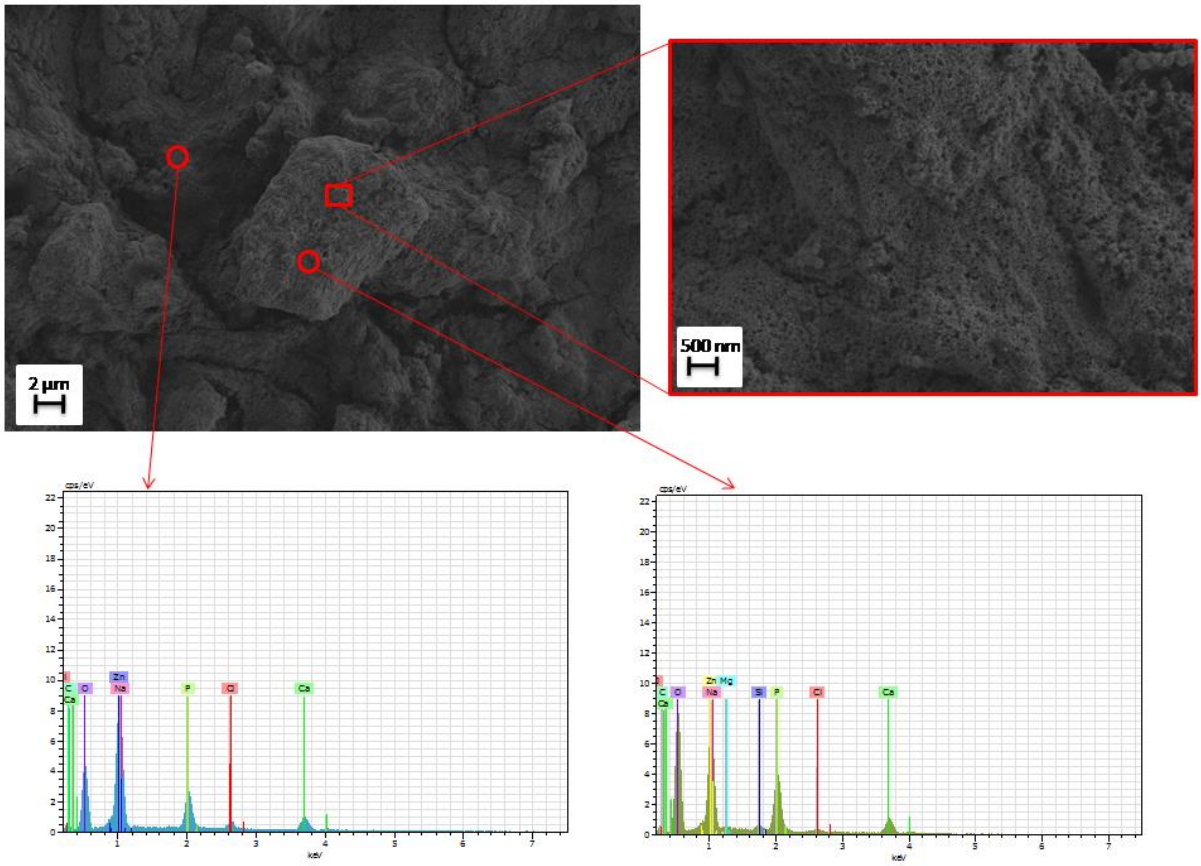

Fig. 10. SEM-EDS analysis of the nZBAP coating after 2 days in SBF solution.

3.6 Antibacterial test

Antibacterial activity of both coatings, nZAPC and nZBAPC, was evaluated against gram-negative *S. aureus* and gram-positive *S. enterica*, and compared with reference untreated stainless steel. The results on colony forming units per milliliter (CFU/ml) after 1 hour incubation of bacterial inoculums on tested surfaces are presented in Fig. 11. For reference and control incubation in inoculums without bacteria was done. No bacterial development was observed for control samples. A significant reduction of bacterial growth (both tested strains), in relation to the reference, was observed after inoculums incubation on nZAPC sample. This data indicates the antimicrobial properties of nZnO particles in combination with the organic matrix of the coating, which is in agreement with previous findings [25]. In contrast, bacterial growth after 1 h incubation on nZBAPC sample increased

ACCEPTED MANUSCRIPT

compared to the reference. Relatively low concentration of BG and ZnO in the nZBAPC coating, as well as the presence of the polymer embedding molecules could cause the lack of antibacterial effect in this sample. Additionally, high surface area, due to the presence of micrometer sized BG particles, can provide suitable niches for bacterial attachment and overcome the antimicrobial activity of zinc oxide and BG. Surface roughness is one of the key parameters determining bacterial attachment [51]. In case of medical devices, implanted materials provide large surface for bacteria to attach and develop biofilm, causing severe infections often resistant to the host defense mechanism and antibiotic treatment [52].

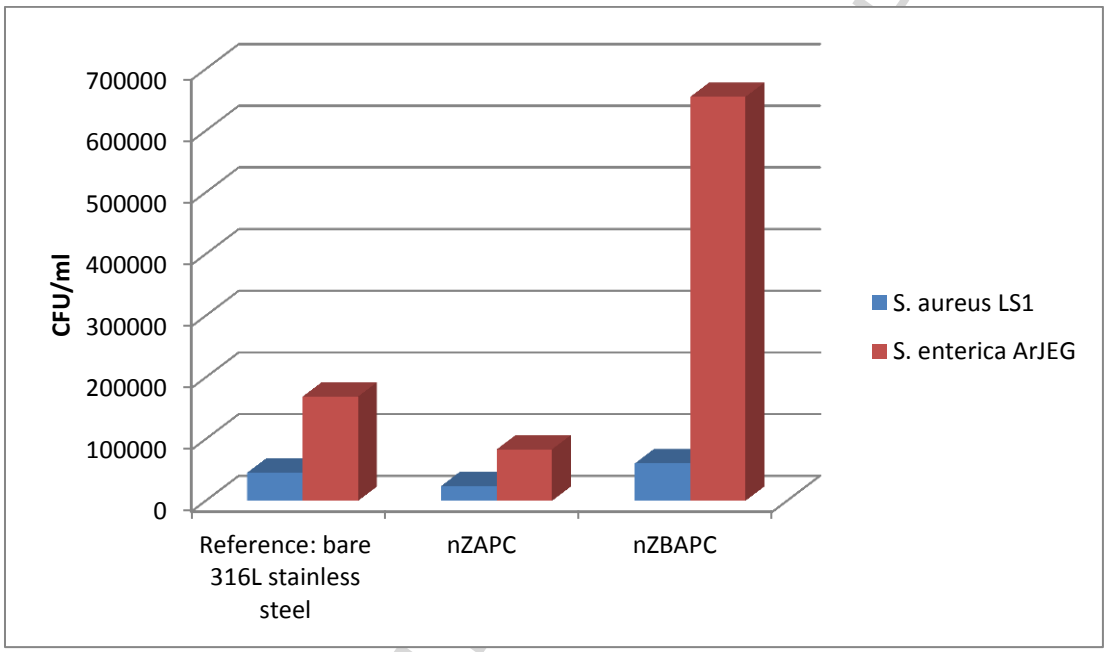

Fig. 11. Antibacterial tests results for *S. aureus* and *S. enteric* bacteria

4. Conclusion

In this study complex organic/inorganic coatings containing nZnO particles were successfully deposited for the first time on stainless steel substrate by EPD. Coatings with incorporated nZnO had antibacterial activity against gram-positive and gram-negative bacteria and increased corrosion resistance compared to the bare substrate. The addition of BG particles resulted in improved *in vitro* bioactivity of the coating, however the high reactivity of BG negatively affected other properties. The advantages of EPD to deposit this type of organic-inorganic composite coatings were demonstrated. However more work is needed to adjust the combination and concentration of the components for achieving an optimal performance of the coatings in terms of reducing the risk of bacterial adhesion while promoting osseointegration.

ACCEPTED MANUSCRIPT

5. Acknowledgement

J. Karbowniczek thanks the European Virtual Institute on Knowledge based Multifunctional Materials (KMM-VIN) for the fellowship to spend a research period at the Institute of Biomaterials, University of Erlangen-Nuremberg, Germany. Luis Cordero acknowledges a full scholarship from the German Academic Exchange Service (DAAD).The authors acknowledge Samira Tansaz for the experimental support and Intrinsiq Materials Ltd (UK) for supplying the nZnO particles.

References

[1] R.B. Heimann, Structure, properties, and biomedical performance of osteoconductive bioceramic coatings, Surf. Coat. Technol. 233 (2013) 27–38.

[2] M. Geetha, A.K. Singh, R. Asokamani, A.K. Gogia, Ti based biomaterials , the ultimate choice for orthopaedic implants – A review, Prog. Mater. Sci. 54 (2009) 397–425.

[3] Q. Chen, G.A. Thouas, Metallic implant biomaterials, Mater. Sci. Eng. R 87 (2015) 1–57.

[4] M. Long, H.J. Rack, Titanium alloys in total joint replacement - a materials science perspective, Biomaterials 19 (1998) 1621–1639.

[5] E. Moran, I. Byren, B.L. Atkins, The diagnosis and management of prosthetic joint infections, J. Antimicrob. Chemother. 65 (2010) 45–54.

[6] J.M. Arduino, K.S. Kaye, S.D. Reed, S.A. Peter, D.J. Sexton, L.F. Chen, N.C. Hardy, S.Y.C. Tong, S.S. Smugar, V.G. Fowler Jr, D.J. Anderson, *Staphylococcus aureus* infections following knee and hip prosthesis insertion procedures, Antimicrob. Resist. Infect. Control. 4 (2015) 1–7.

[7] J. Hasan, R.J. Crawford, E.P. Ivanova, Antibacterial surfaces: the quest for a new generation of biomaterials, Trends Biotechnol. 31 (2013) 295–304.

[8] L. Zhao, P.K. Chu, Y. Zhang, Z. Wu, Review antibacterial coatings on titanium implants, J. Biomed. Mater. Res. Part B Appl. Biomater. 91B (2009) 470–480.

[9] S. Radin, J.T. Campbell, P. Ducheyne, J.M. Cuckler, Calcium phosphate ceramic coatings as carriers of vancomvcin, Biomaterials 18 (1997) 777–782.

[10] S. Radin, P. Ducheyne, Controlled release of vancomycin from thin sol – gel films on titanium alloy fracture plate material, Biomaterials 28 (2007) 1721–1729.

[11] O.P. Edupuganti, V. Antoci, S.B. King, B. Jose, C.S. Adams, J. Parvizi, I.M. Shapiro, A.R. Zeiger, N.J. Hickok, E. Wickstrom, Covalent bonding of vancomycin to Ti6Al4V alloy pins provides long-term inhibition of *Staphylococcus aureus* colonization, Bioorganic Med. Chem. Lett. 17 (2007) 2692–2696.

[12] D. Teker, F. Muhaffel, M. Menekse, N. Gul, M. Baydogan, H. Cimenoglu, Characteristics of multi-layer coating formed on commercially pure titanium for biomedical applications, Mater. Sci. Eng. C 48 (2015) 579–585.

[13] W. Chen, Y. Liu, H.S. Courtney, M. Bettenga, C.M. Agrawal, J.D. Bumgardner, J.L. Ong, In vitro anti-bacterial and biological properties of magnetron co-sputtered silver-containing hydroxyapatite coating, Biomaterials 27 (2006) 5512–5517.

[14] H. Jeon, S.-C. Yi, S.-G. Oh, Preparation and antibacterial effects of Ag – SiO_2 thin films by sol – gel

ACCEPTED MANUSCRIPT

method, Biomaterials 24 (2003) 4921–4928.

[15] A. Ewald, S.K. Glückermann, R. Thull, U. Gbureck, Antimicrobial titanium/silver PVD coatings on titanium, Biomed. Eng. Online 10 (2006) 1–10.

[16] K. Ryong, S. Il, Y. Gun, D. Hyuk, Deposition of hydroxyl-apatite on titanium subjected to electrochemical plasma coating, Electrochim. Acta 109 (2013) 173–180.

[17] M. Miola, E. Vernné, F.E. Ciraldo, L. Cordero-Arias, A.R. Boccaccini, Electrophoretic deposition of chitosan/45S5 bioactive glass composite coatings doped with Zn and Sr, Front. Bioeng. Biotechnol. 3 (2015) 1–13.

[18] S. Seuss, M. Lehmann, A.R. Boccaccini, Alternating current electrophoretic deposition of antibacterial bioactive glass-chitosan composite coatings, Int. J. Mol. Sci. 15 (2014) 12231–12242.

[19] L. Besra, M. Liu, A review on fundamentals and applications of electrophoretic deposition (EPD), Prog. Mater. Sci. 52 (2007) 1–61.

[20] Q. Chen, L. Cordero-Arias, J.A. Roether, S. Cabanas-Polo, S. Virtanen, A.R. Boccaccini, Alginate/Bioglass ® composite coatings on stainless steel deposited by direct current and alternating current electrophoretic deposition, Surf. Coat. Technol. 233 (2013) 49–56.

[21] D. Zhitomirsky, J.A. Roether, A.R. Boccaccini, I. Zhitomirsky, Electrophoretic deposition of bioactive glass/polymer composite coatings with and without HA nanoparticle inclusions for biomedical applications, J. Mater. Process. Technol. 9 (2008) 1853–1860.

[22] T. Moskalewicz, M. Kot, S. Seuss, A. Kędzierska, A. Czyrska-Filemonowicz, A.R. Boccaccini, Electrophoretic deposition and characterization of HA/Chitosan nanocomposite coatings on Ti6Al7Nb alloy, Met. Mater Int. 21 (2015) 96–103.

[23] F. Sun, X. Pang, I. Zhitomirsky, Electrophoretic deposition of composite hydroxyapatite – chitosan – heparin coatings, J. Mater. Process. Technol. 209 (2008) 1597–1606.

[24] F. Pishbin, V. Mouriño, J.B. Gilchrist, D.W. McComb, S. Kreppel, V. Salih, M.P. Ryan, A.R. Boccaccini, Single-step electrochemical deposition of antimicrobial orthopaedic coatings based on a bioactive glass/chitosan/nano-silver composite system, Acta Biomater. 9 (2013) 7469–7479.

[25] L. Cordero-Arias, S. Cabanas-Polo, O.M. Goudouri, S.K. Misra, J. Gilabert, E. Valsami-Jones, E. Sanchez, S. Virtanen, A.R. Boccaccini, Electrophoretic deposition of ZnO/alginate and ZnO-bioactive glass/alginate composite coatings for antimicrobial applications, Mater. Sci. Eng. C 55 (2015) 137–144.

[26] R. Meraat, A. Abdolahzadeh Ziabari, K. Issazadeh, N. Shadan, K. Mazloum Jalali, Synthesis and characterization of the antibacterial activity of zinc oxide nanoparticles against *Salmonella typhi,* Acta Metall. Sin. (Engl. Lett.), 29 (2016) 601–608.

[27] S.C. Esparza-González, S. Sánchez-Valdés, S.N. Ramírez-Barrón, M.J. Loera-Arias , J.Bernal, H. Iván Meléndez-Ortiz, R.Betancourt-Galindo, Effects of different surface modifying agents on the cytotoxic and antimicrobial properties of ZnO nanoparticles, Toxicol. In Vitro, 37 (2016) 134-141.

[28] A. Sirelkhatim, S. Mahmud, A. Seeni, N.H.M. Kaus, L.C. Ann, S.K.M. Bakhori, H. Hasan, D. Mohamad, Review on zinc oxide nanoparticles: antibacterial activity and toxicity mechanism, Nano-Micro Lett. 7 (2015) 219–242.

[29] C. Silvestre, D. Duraccio, A. Marra, V. Strongone, S. Cimmino, Development of antibacterial composite films based on isotactic polypropylene and coated ZnO particles for active food packaging, Coatings 6 (2016) 1-14.

[30] R. Venkatesan, N. Rajeswari, ZnO/PBAT nanocomposite films: Investigation on the mechanical and biological activity for food packaging, Polym. Adv. Technol. 28 (2017) 20-27.

ACCEPTED MANUSCRIPT

[31] J. T. Seil, T. J. Webster, Reduced Staphylococcus aureus proliferation and biofilm formation on zinc oxide nanoparticle PVC composite surfaces, Acta Biomater. 7 (2011) 2579–2584.

[32] L.L. Hench, Biomaterials : a forecast for the future, Biomaterials 19 (1998) 1419–1423.

[33] Q. Chen, L. Cordero-Arias, J.A. Roether, S. Cabanas-Polo, S. Virtanen, A.R. Boccaccini, Alginate/Bioglass® composite coatings on stainless steel deposited by direct current and alternating current electrophoretic deposition, Surf. Coatings Technol. 233 (2013) 49–56.

[34] L. Cordero-Arias, S. Cabanas-Polo, J. Gilabert, O. M. Goudouri, E. Sanchez, S. Virtanen, A.R. Boccaccini, Electrophoretic deposition of nanostructured TiO_2/alginate and TiO_2-bioactive glass/alginate composite coatings on stainless steel, Adv. Appl. Ceram. 113 (2014) 42–49.

[35] X. Pang, I. Zhitomirsky, Electrophoretic deposition of composite hydroxyapatite-chitosan coatings, Mater. Charact. 58 (2007) 339–348.

[36] L. Cordero-Arias, S. Cabanas-Polo, H. X. Gao, J. Gilabert, E. Sanchez, J.A. Roether, D.W. Schubert, S. Virtanen, A.R. Boccaccini, Electrophoretic deposition of nanostructured-TiO_2/chitosan composite coatings on stainless steel, RSC Adv. 3 (2013) 39–41.

[37] P. Stadelmann, “JEMS Java Electron Microscopy Software,” 2004.

[38] T. Kokubo, Apatite formation on surfaces of ceramics, metals and polymers in body environment, Acta Mater. 46 (1998) 2519–2527.

[39] M.E. Olson, K.L. Garvin, P.D. Fey, M.E. Rupp, Adherence of *Staphylococcus epidermidis* to Biomaterials Is Augmented by PIA, Clin. Orthop. Relat. Res. 451 (2006) 21–24.

[40] I. Yoda, H. Koseki, M. Tomita, T. Shida, H. Horiuchi, H. Sakoda, M. Osaki, Effect of surface roughness of biomaterials on *Staphylococcus epidermidis* adhesion, BMC Microbilogy 14 (2014) 1–7.

[41] H.H. Lu, S.R. Pollack, P. Ducheyne, Temporal zeta potential variations of 45S5 bioactive glass immersed in an electrolyte solution, J. Biomed. Mater. Res. 51 (2000) 80–87.

[42] B. Wind, E. Killmann, Adsorption of polyethylene oxide on surface modified silica – stability of bare and covered particles in suspension, Colloid Polym. Sci. 276 (1998) 903–912.

[43] N.S. Labidi, A. Djebaili, Studies of the mechanism of polyvinyl alcohol adsorption on the calcite/water interface in the presence of sodium oleate, J. Miner. Mater. Charact. Eng. 7 (2008) 147–161.

[44] Q. Chen, S. Cabanas-Polo, O.M. Goudouri, A.R. Boccaccini, Electrophoretic co-deposition of polyvinyl alcohol (PVA) reinforced alginate-Bioglass® composite coating on stainless steel: mechanical properties and in-vitro bioactivity assessment, Mater. Sci. Eng. C 40 (2014) 55–64.

[45] M. Wisniewska, The temperature effect on electrokinetic properties of the silica – polyvinyl alcohol (PVA) system, Colloid. Polym. Sci, 289 (2011) 341–344.

[46] V. Mouriño, P. Newby, A.R. Boccaccini, Preparation and characterization of gallium releasing 3-D alginate coated 45S5 bioglass® based scaffolds for bone tissue engineering, Adv. Eng. Mater. 12 (2010) B283–B291.

[47] S. Sudhamani, M.Prasad, K.U. Sankar, DSC and FTIR studies on gellan and polyvinyl alcohol (PVA) blend films, Food Hydrocoll. 17 (2003) 245–250.

[48] J. Kumar S.F. D’Souza, Preparation of PVA membrane for immobilization of GOD for glucose biosensor., Talanta 75 (2008) 183–188.

[49] G. Xiong, U. Pal, J.G. Serrano, K.B. Ucer, R.T. Williams, Photoluminescence and FTIR study of ZnO nanoparticles: the impurity and defect perspective, Phys. Status Solidi C 3 (2006) 3577–3581.

[50] O.P. Filho, G.P. La Torre, L.L. Hench, Effect of crystallization on apatite-layer formation of bioactive glass 45S5, J. Biomed. Mater. Res. 30 (1996) 509–514.

ACCEPTED MANUSCRIPT

[51] M. Lorenzetti, I. Dogsa, T. Stosicki, D. Stopar, M. Kalin, S. Kobe, S. Novak, The Influence of Surface Modification on Bacterial Adhesion to Titanium-Based Substrates, ACS Appl. Mater. Interfaces 7 (2015) 1644–1651.

[52] M. Katsikogianni, Y.F. Missirlis, Concise review of mechanisms of bacterial adhesion to biomaterials and of techniques used in estimationg bacteria-material interactions, Eur. Cells Mater. 8 (2004) 37–57.

ACCEPTED MANUSCRIPT

ACCEPTED MANUSCRIPT

Highlights

- Organic-inorganic composite coatings produced by electrophoretic deposition
- Antibacterial ZnO nanoparticles incorporated in alginate coatings
- Bioactive glass added to impart bioactivity in multifunctional coatings

ACCEPTED MANUSCRIPT